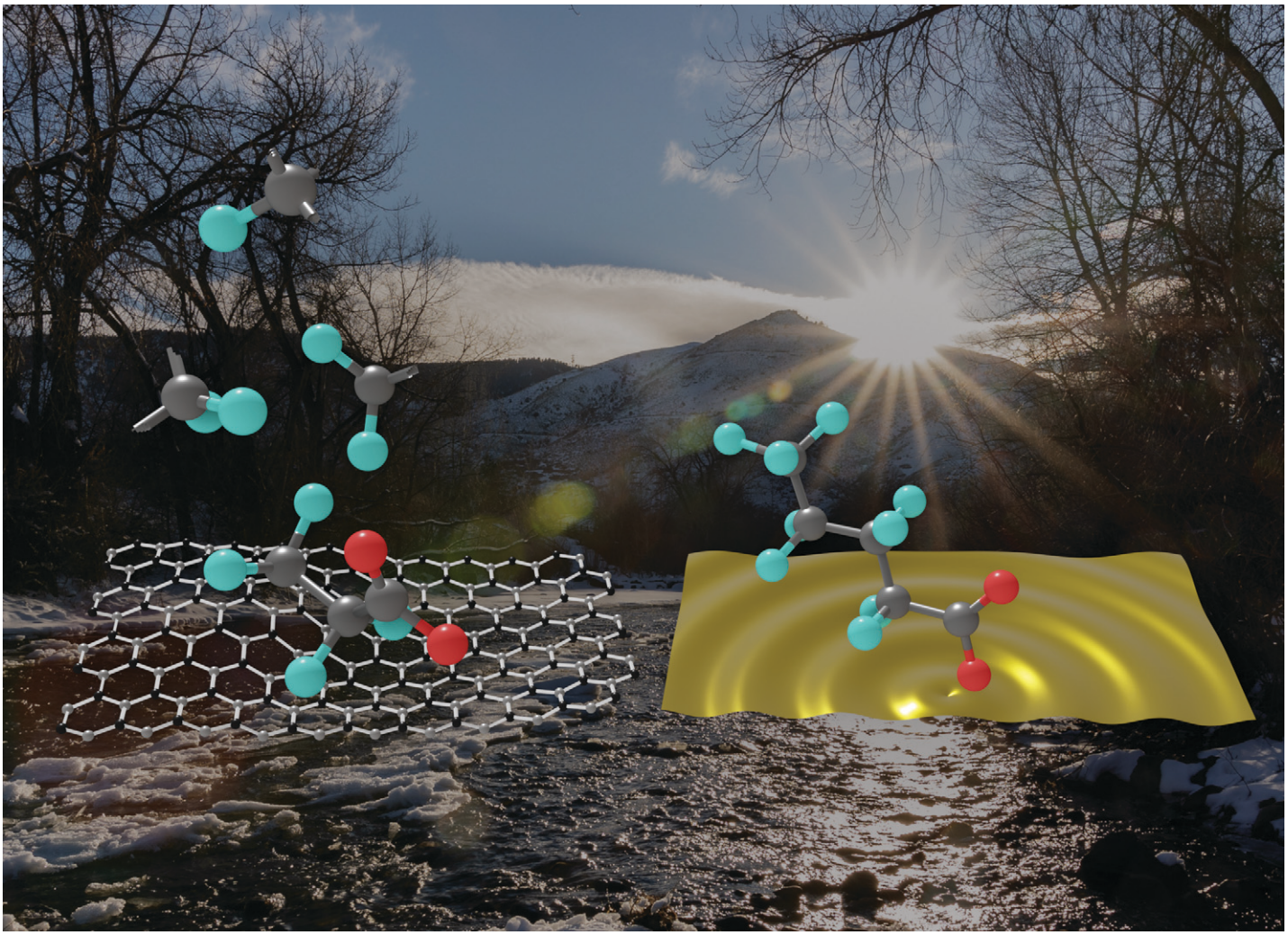

Showcasing research from the Richards, Trewyn & Vyas Research Groups, School of Chemistry, Colorado School of Mines, United States.

Light-driven interfaces for polyfluoroalkyl substances (PFAS) detection and destruction

The Richards, Trewyn, and Vyas research groups at the Colorado School of Mines are developing innovative methods for per- and polyfluoroalkyl substance (PFAS) remediation. By integrating materials science, organic chemistry, and computational tools, they aim to create the next generation of PFAS degradation materials. This article highlights recent advancements in light-driven technologies for PFAS detection and destruction. New developments in photocatalysis are improving the efficiency of degrading these persistent chemicals, while plasmonic materials are proving effective for detecting PFAS, especially as detection targets become lower and harder to measure. Key features that contribute to the success of these materials are also discussed to guide future developments.

Image reproduced by permission of Colorado School of Mines

As featured in:

See Brian G. Trewyn, Shubham Vyas, Ryan M. Richards *et al.*, *RSC Appl. Interfaces*, 2024, **1**, 833.

ROYAL SOCIETY OF CHEMISTRY

rsc.li/RSCApplInter

Registered charity number: 207890

RSC Applied Interfaces

ROYAL SOCIETY OF CHEMISTRY

REVIEW

View Article Online
View Journal | View Issue

Cite this: *RSC Appl. Interfaces*, 2024, 1, 833

Light-driven interfaces for PFAS detection and destruction

Frank R. A. Schrama, Scott E. Massimi, Michael R. Dooley, Brian G. Trewyn,* Shubham Vyas* and Ryan M. Richards*

Due to exposure risks and health concerns, global limitations on per- and polyfluoroalkyl substances (PFAS) have become increasingly restrictive over the last few years, with limitations of some legacy PFAS in drinking water reaching single digit ppt in the United States and certain European countries. As the allotted maxima for contamination have reached such low levels, broad research efforts in the degradation and detection of PFAS materials are being intensely investigated. Light driven technologies (photocatalysis and plasmonics) represent important interfacial phenomena with potential to detect and/or decompose PFAS. Despite the commonalities at the interface, little discussion merging detection and destruction exists, thereby resulting in minimal transference of concepts, experimental success, and potential dual functionality systems. This review will cover the basics of photocatalytic degradation technologies surrounding PFAS, the basics of plasmonics for PFAS detection, and a discussion on how these fields can progress in future work.

Received 15th May 2024,
Accepted 4th July 2024

DOI: 10.1039/d4lf00171k

rsc.li/RSCApplInter

1. Introduction

As scrutiny on the release of per- and polyfluoroalkyl substances (PFAS) into the environment and contamination of all environmental matrices has increased over the years, so too have the breadth of technologies being investigated to mitigate, capture, and/or destroy PFAS pollutants.[1,2] This increased scrutiny is due to the numerous adverse health impacts associated with PFAS exposure including several forms of cancer and connections to birth defects.[3–8] This negative impact on health is partially due to the long half-life of PFAS within the human body, and the half-life of PFAS under oceanic conditions is around 250 years, thus, the longevity of these pollutants is significant for future generations.[9] Preventative technologies that have been investigated so far include electrochemical oxidation, plasma treatment, oxidative and reductive photocatalysis, sonolysis, supercritical water oxidation, hydrothermal alkaline treatment and thermal degradation.[1]

PFAS materials are known for their unique chemical features, namely their hydrophobic and oleophobic nature, high stability in ambient environments, and resistance to degradation *via* oxidation and reduction pathways. These features result in a material which offers many utilitarian advantages as a protective or preventative layer that has been used in paints, non-stick cookware, cleaning products, fire-resistant and fire dousing materials, and many more.[10–12] While the uses of PFAS have been ongoing for over half a century,[13] the harmful effects of these materials have only been investigated in recent times. Legacy PFAS, such as perfluorooctanoic acid (PFOA) and perfluorooctanesulfonic acid (PFOS), have been deemed toxic and pervasive within the human body, causing them to be phased out of production over the years.

While it is generally the unique properties of PFAS that make them difficult to remove from the environment, researchers are attempting to exploit these same properties to help remove these materials from our environment. For example, as PFAS molecules have a hydrophilic head group and a hydrophobic tail, they tend to aggregate onto interfaces. Materials have been designed to take advantage of this behaviour, for example the capture of PFAS onto granular activated carbon or *via* foam fractionation techniques.[14,15] By designing materials that PFAS readily adsorb to and which

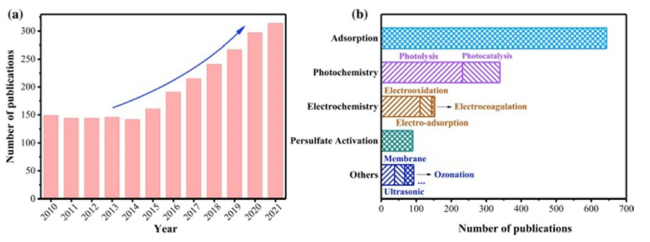

Fig. 1 A notable increase in PFAS destruction and removal technologies can be seen in the last decade. A large portion of these is associated with photolysis and photocatalysis.[16]

Department of Chemistry, Colorado School of Mines, Golden, CO 80401, USA. E-mail: btrewyn@mines.edu, svyas@mines.edu, rrichard@mines.edu

serve a specific function, such as materials that can degrade recalcitrant materials near their surface, additional optimization *via* leveraging the nature of PFAS can be achieved. Finally, intelligent material design can go one step further by creating materials that are able to adsorb and interact with PFAS yet require little energetic input, such as the light interacting materials presented in this review.

A recent review summarized the types of PFAS degradation strategies prevalent in the literature as seen in Fig. 1.[16] Technologies based on light, such as photocatalysis for PFAS destruction, are promising due to their unique benefits, such as having relatively low energy consumption compared to thermal treatments, end-products that are typically less- or non-harmful, the ability to target multiple pollutants in wastewater, the capability to be used in both aqueous and gaseous phases, and typical mild reaction condition requirements with reasonable reaction kinetics, to mention a few.[17] With significant advancements in UV-light treatment technology, commonly employed in water treatment plants for organic pollutant removal, photocatalytic degradation methods could leverage existing infrastructure, leading to simpler implementations compared to some other methods.[18]

Due to the increased concerns of PFAS toxicity in recent years, the suggested PFAS concentration levels in drinking water have decreased significantly (for example, PFOA limits have been set as low as 4 ppt in April 2024).[19,20] As a result, there is an urgent need to develop detection methods capable of measuring PFAS at these extremely low concentrations that can be utilized on-site at water treatment plants with rapid response times. While the traditional methods such as liquid chromatography mass spectrometry (LC-MS) can reach low concentration limits of quantification (LOQ), the low mobility and long run-times of the said methods in addition to the initial cost of instrumentation are often inefficient for testing of water at treatment plants on a national scale.

A different light-driven technology which has gained increased traction is plasmonic driven photo-detectors for bio(chemical) systems.[21–24] These detectors have increased mobility for portable, on-site testing applications, offer quick response times, and have demonstrated significant improvement over the last decade in the LOQ concentrations they can achieve.[25] Alternatively, efforts are also ongoing for PFAS detection *via* electrochemistry based sensing approaches. However, significant research is still needed to improve the sensitivity and selectivity of such methods.[26–28]

In recent decades, the technology of plasmonic sensors has been advanced *via* the addition of optical fibres, used to improve the spatial resolution and detection limits.[29,30] The use of plasmonic sensors is based on the property that all materials have a unique diffraction angle when hit with an incident light source. A surface layer of pre-defined receptors is designed and deposited on a gold (Au) film, which will have a specific angle of incidence as light reflects off the surface. If the specific binding sites on top of the gold surface bind to the analyte, the overall system changes, resulting in the specific angle of reflection to shift. The appearance of this shift indicates the presence of the analyte, and as the technology improves, the extent of the shift can be correlated to the concentration of the analyte (Fig. 2).[31]

In terms of degradation, there have been many recent developments in photocatalytic materials capable of destroying PFAS. These materials come in a wide variety and are able to trap PFAS in a reactive environment after the target binds to the surface and the material is excited. These materials are a promising direction for degradation efforts.

In this review, we strive to provide an overview of the two predominant light-driven technologies utilized in the decomposition and detection of PFAS materials, namely semiconductor photocatalysts for degradation and plasmonic photo-sensors for the detection of PFAS. This review aims to discuss these topics under the lens of the surface functionality that can be utilized for PFAS. As this review focusses on photocatalysis and plasmonic materials due to their similar light interactions, other pertinent light-based detection methods, such as fluorescence,[32] Raman and resonance scattering,[33] and UV-detection,[34] can be found in the respective review papers provided.

2. Plasmonic materials

Plasmonic materials, also sometimes termed nanoplasmonics, are sensitive to the frequencies of the IR and visible light spectra when irradiated along the dielectric surface. Surface plasmonic materials have found utility in a variety of environmental remediation technologies. Due to the capabilities of plasmonic materials to act as hot electron generators, they have demonstrated application in near-surface heat transfer, enhancements for absorbers, emitters, and reflectors, and enhancement for photocatalytic processes, as well as other technologies.[35] Included in these are the detection and destruction of environmental pollutants, including recalcitrant organics.[36,37] A large focus of the work done on plasmonic materials with respect to PFAS surrounds specific PFAS detection at ultra-low concentrations.

Recently, the United States Environmental Protection Agency (USEPA) implemented a regulation concerning the

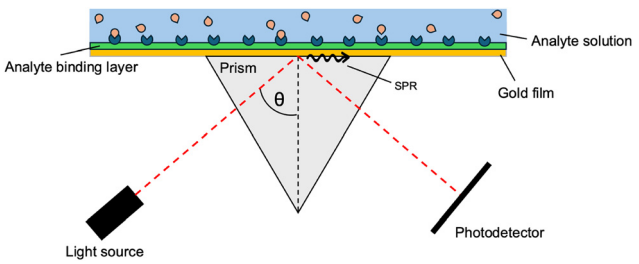

Fig. 2 Depiction of the SPR sensor technology in a Kretschmann configuration. A specific angle of reflectance will instigate SPR, causing a decrease in measured light intensity. As the analyte binds, the angle at which SPR occurs will shift. This figure was created by the authors.

maximum contamination level of PFOA and PFOS to be 4 ppt in drinking water with other countries setting lower limits (*e.g.* Denmark setting the limit for certain PFAS to 2 ppt).[38] In an effort to achieve sufficient PFAS detection, one potential solution is the use of plasmonic sensors. In general, plasmonic sensors work *via* measuring the angle of incident light at which surface plasmon resonance (SPR) occurs by measuring a decrease in reflected light intensity. As the analyte binds to the reflective material (typically gold), the specific angle at which SPR occurs shifts and this shift is noted as the presence of the analyte. A more detailed description of this effect is discussed in section 2.2 SPR fibre-optic sensors. As plasmonic detectors become more mobile, analyte specific, and become easier to use, their potential use for on-site testing of toxic PFAS substances becomes more possible.

2.1 Light interactions with plasmonic materials

Plasmonic materials function *via* the generation of plasmons, which are the collective oscillations of the free electron cloud activated *via* light. Plasmons can be considered as bosonic quasiparticle excitations. Bosonic quasiparticles refer to the fact that while individual electrons act as fermions (clear separation between each particle), the synchronous oscillation of the electron cloud can be considered to act as if it were one particle (quasiparticle), with the components free to stack upon themselves (bosonic). Within the bulk of plasmonic materials, the generation of plasmons occurs *via* a direct electron beam; however, excitation *via* electromagnetic radiation or light is not allowed. This is due to the energy dispersion curves of photons and plasmons not crossing when in bulk. On the surface of these materials however there can exist an electromagnetic radiation driven excitation of the free electron cloud, resulting in the displacement of the free electron cloud with respect to the stationary positive ion lattice. This excitation results in propagating surface plasmon polaritons (PSPPs) which propagate across along with the light wave (Fig. 3).[39,40]

In certain cases, metallic nanoparticles (NPs) such as gold can induce a type of surface plasmon different than the PSPPs. If the total size of the NPs is similar to that of the skin-depth surface, (ergo before a significant bulk-depth is reached), and the NP size is significantly smaller than the wavelength of the incident light, the NPs can generate plasmons throughout the whole volume of the material.[39] Due to the entire volume of the particle participating in the generation of the plasmon, no propagation is able to take place within the material resulting in localized surface plasmons (LSPs) or localized surface plasmon resonance (LSPR). As the generated plasmons involve the whole of the particles, a dipole is formed over the entire material of stationary positive ions and the oscillating free electron cloud, which collectively act as a mass–spring harmonic oscillator. If the incident light wave is of a wavelength which is in resonance with the oscillation of the electron cloud, the LSP can be formed. The generated plasmon system is also known as a surface plasmon resonance (SPR) system. Once the plasmon is generated within the NP, electron relaxation occurs *via* multiple pathways. The predominant pathway of energy loss is *via* intraband transitions. In the example of gold NPs, which have been extensively researched as plasmonic materials due to their relatively facile plasmon generation ability combined with chemical stability, the energy loss of the LSP occurs mainly through the intraband excitation of 5d orbital electrons into the unoccupied 6s–p orbitals, generating electron–hole pairs.[39] This energy loss from the LSP eventually dissipates as heat, resulting in highly condensed regions of intense heat that have been studied as pollutant degradation technologies *via* thermal dispersion and *via* the generation of hot electrons (Fig. 4).[36,40,41]

2.2 SPR fibre-optic sensors

In a SPR system, there exists an angle of the incident light where the light wave vector is in resonance with the dielectric/metal surface plasmons, which is known as the SPR angle (θ_{SPR}). The PSPP on the surface is very sensitive to the dielectric properties of the system, enabling sensory detection methods. These detection methods are angular-modulated, wavelength-modulated, or intensity-modulated, with angular-modulated systems being the most common and sensitive. In the angular-modulated system, a monochromatic beam of light is directed towards the dielectric/surface interface with the angle of incidence changing over time. Any changes to

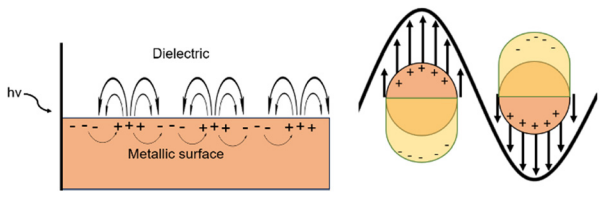

Fig. 3 A simplified diagram of PSPPs (left) and LSPs (right) when light interacts with either the surface of a bulk metal or nanoparticles. This figure was created by the authors.

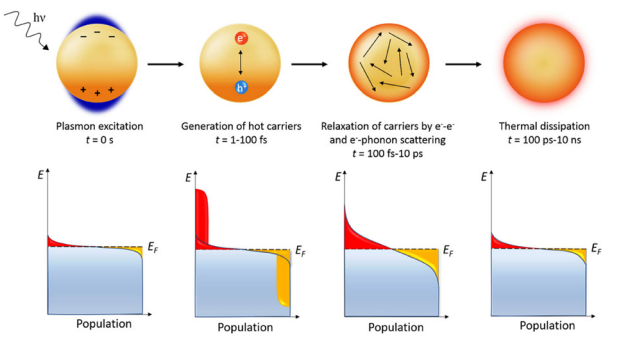

Fig. 4 Plasmon induced hot hole generation resulting in thermal dissipation with time frames.[40]

the dielectric/surface interface will result in a shift in the θ_{SPR}, noted as a shift in the wavelength at which reflected light intensity drops.[37]

A simple modification to the metal can be used to allow detection of specific materials. By attaching binding sites for the target analyte onto the opposite end of the metal surface (see Fig. 5(a)), a shift in the characteristic θ_{SPR} can be seen, as shown in Fig. 5(b). As the analyte of interest is introduced into the system, the binding sites become increasingly occupied, causing a further shift in the θ_{SPR} until reaching a binding–unbinding equivalence point for the corresponding analyte concentration (see Fig. 5(c)). Using this binder–analyte property, low concentrations of analyte can be measured within complex matrices. The main concern for θ_{SPR} analysis is non-analyte molecules causing false positives by attaching to binding sites.

In the literature, the SPR technology used for PFAS is mainly focused on probing. As the allowed concentration of PFAS is set on the scale of a few parts per trillion, a surge of analytical techniques has appeared to meet the low LOQ required for sufficient testing. The current state-of-the-art technologies for ultra-low PFAS concentrations are LC-MS and gas chromatography-mass spectroscopy (GC-MS), with other techniques currently investigated including capillary zone electrophoresis (CZE), colorimetric sensors, fluorous membrane-based ion-selective electrodes, fluorescence-based sensors, electrochemical impedance spectroscopy (EIS), impedance sensors, and ion-transfer stripping voltammetry.[25] These techniques all require expensive equipment and are often non-portable, require high levels of user training, and are time consuming in both the instrumental analysis and the analyte preparation.[25]

SPR-based sensing technologies aim to circumvent these challenges while still providing an accurate detection method for ppt levels of PFAS concentrations. A limitation of SPR-POFs (plastic optical fibres) is that SPR surface binding to the analyte has used bioreceptors, resulting in the detection of low concentrations (LOD-limit of detection around 0.2 ppb), but not ultra-low concentrations. Recently, attempts have been made to improve on the SPR system by replacing the bioreceptors on the SPR-POF system with molecular imprinted polymers (MIPs), specifically targeting PFOA.[25] MIPs have similar selectivity and specificity as bioreceptors while being more stable and having more facile production steps. The authors showed that MIP addition lowered the LOD to 0.81 ppt, which falls within the extreme low concentrations required for legacy PFAS limits. Their testing included an analysis of a simulated sea water matrix which was spiked with known amounts of PFOA. The results shown in Fig. 6 indicated that the SPR-MIP sensor setup was able to detect small changes in PFOA concentration within a more complex matrix, with a notable shift in the SPR angle θ_{SPR} with each subsequent increase in PFOA concentration.

As a measure of responsivity for the SPR-MIP sensor, the authors used a Langmuir fitting of the change in the observed wavelength ($\Delta\lambda$ nm) compared to the PFOA concentration at the ppt level and noted that compared to the Langmuir fitting of the sensor in Milli-Q water, the performance was reduced when placed in a more complex matrix. The authors attributed this decrease in performance to the chloride anions in the seawater matrix binding to the vinylbenzyl trimethylammonium chloride monomers within the MIP, where an equilibrium state is reached between PFOA and the chloride anions. This competition results in lower sensitivity in the probe readings.

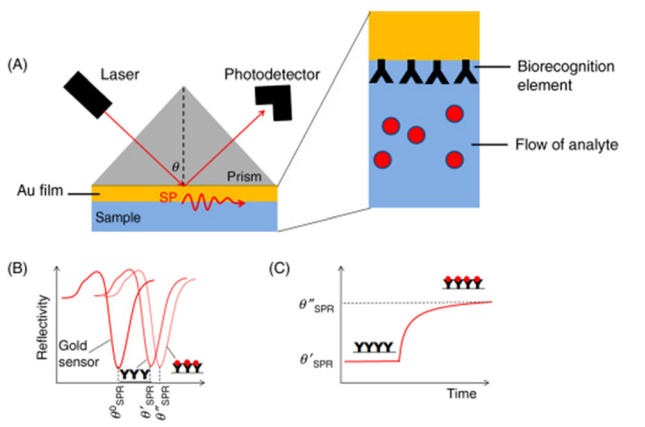

Fig. 5 Example of SPR sensing technology. As the analyte binds onto the sensor's surface (a), a shift in the incident angle for SPR is noted (b), indicating that the analyte is present. As more analyte binds, the change in angle levels off (c).[37] This figure has been modified from its original publication.

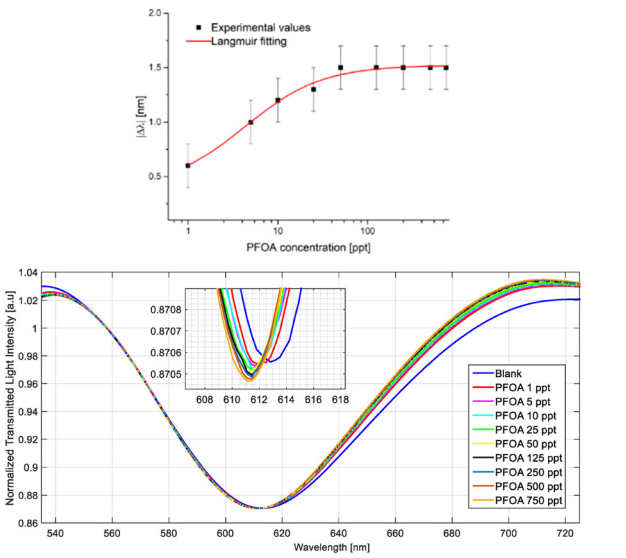

Fig. 6 Test results by Pitruzzella *et al.* for their MIP sensor within a simulated seawater matrix. The data readings (top) combined with the noted change in the observed wavelength with increasing concentration (bottom) indicate that the sensitivity of the sensor decreases with higher concentrations.

2.3 Plasmonic devices for light driven PFAS degradation

Plasmonic devices have been used in a variety of technologies including the degradation of organic pollutants, catalysis *via* direct electron transfer, sensing, and others.[25,36,40–42] Due to the generation of highly energetic hot carriers within the plasmonic system, potential degradation pathways are made possible. For example, generated hot electrons within plasmonic systems are theoretically able to undergo a similar photo-oxidative degradation mechanism to that of other photocatalysts mentioned earlier.

More research is required in the field of plasmonic-driven degradation of PFAS materials to determine the optimal parameters, whether the system should be designed as an oxidative photocatalyst, a photoelectrochemical system, or a reductive photocatalyst *via* generated 'hot-holes'. Fig. 7(a) and (b) show two depictions of surface plasmon induced photocatalysis. In Fig. 7(a), the gold nanoparticle acts as both an electron generator *via* SPR and an electron sink for the titanium dioxide (TiO_2) exciton, which is then able to perform reduction processes, while Fig. 7(b) shows an autonomous solar water-splitting device where the majority of generated electrons come from gold nanoparticles undergoing LSPs *via* light-driven excitation.[35]

With any technology, certain challenges need to be recognized and addressed to improve the field. In the current literature, the main factors which can limit the effectiveness of plasmonic based systems are efficient light absorption, effective and specific surface adsorption for potential analyte destruction, and the ability to generate hot electrons.[36]

Work done in the field of plasmonic catalysis is widespread. A previous study showed that *via* a facile impregnation route, Au nanoparticles (NPs) could be integrated into a TiO_2 anatase and P25 crystal phase. This integration of gold resulted in an anisotropic flow of SPR generated hot electrons from gold NPs within the crystal structure to the edge of the overall TiO_2 crystal, resulting in easily accessible electrons for further reaction and increased recombination times due to the separation of holes and electrons.[43]

More current work in the field shows advancements of plasmonic catalysis for a variety of uses. Recently, it has been demonstrated that a plasmonic nanohybrid system enabled the hydrogen evolution reaction in which plasmonic generated hot electrons would transfer into the nanohybrid system's ligands and facilitate the concerted proton-electron transfer step and promote hydrogen formation.[44]

A recent investigation across multiple studies aimed to elucidate the effect of LSPR generated hot electrons on CO_2 methanation. These studies found that *via* the modification of Ag-doped Ni catalysts,[45] Au-doped Ni catalysts,[46] and TiN-doped Ni catalysts,[47] the generated hot electrons from the plasmonic active materials (Ag, Au, TiN) were able to improve the CO_2 methanation conversion. One recent paper partially ascribes the increased efficiency for the CO_2 methanation *via* Ni to the hot electrons increasing the Ni surface charge, resulting in more strongly bound CO (a competing end-product for the methanation reaction), and as such lowering the amount of CO products to be removed from the Ni surface before full completion of the CH_4 production.[47]

As shown, plasmonic catalysts have been shown to be of use in a variety of catalytic processes. Investigations into the potential uses of plasmonic materials for PFAS degradation *via* photocatalytic means (discussed in section 3 Photocatalytic degradation of PFAS) could be a worthwhile venture into increasing photocatalytic efficiency.

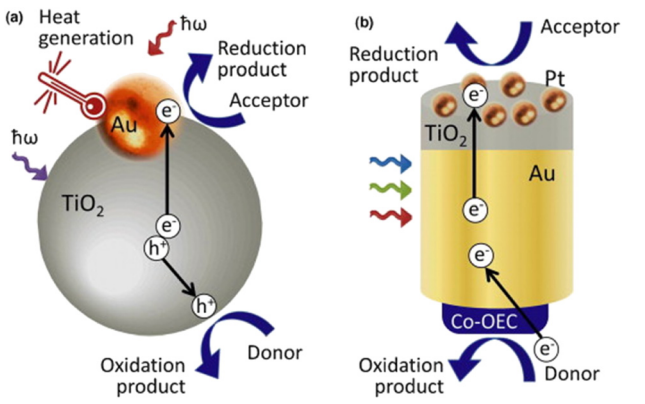

Fig. 7 Examples of non-sensor based plasmonic technologies. (a) Plasmonic gold (Au) nanoparticle acts as an electron sink for excited semiconductor electrons as well as an independent electron generator for a more efficient photoactive catalyst. (b) A collection of gold nanoparticles excited *via* light generates SPR electrons which are then used within the electrochemical cell.[35]

3. Photocatalytic degradation of PFAS

3.1 Photocatalytic activation

A photocatalyst is a type of catalyst which is excited when irradiated by light of a higher energy than the band gap of the material. An electron (e^-) within the catalyst absorbs the energy from the photon and is excited from the valence band to the conduction band. This generates an excited electron within the conduction band (e_{cb}^-) and leaves behind a positive hole in the valence band (h_{vb}^+). The generated charge carriers are then able to drive redox reactions, with electrons driving reduction reactions and holes driving oxidation reactions. However, there are often competing processes that either prevent the desired reactions from taking place or change the reactivity of the excitons. The first of these processes is recombination, or when the excited electron returns to the conduction band, losing the absorbed energy typically through heat or light, and refills the hole. Recombination is generally not desired, and the recombination rate is a good indicator of the efficiency of a photocatalyst. Another process that can occur is referred to as trapping, in which the excited charge carriers are "trapped" in an energy state between the valence band and the conduction band. The middling energy state slows down

the process of recombination, allowing more time for charge carriers to perform redox reactions. In titanium dioxide, defects such as oxygen vacancies provide excellent electron traps, and while these trapped electrons are generally less reactive, the holes that would otherwise be quenched by the trapped electrons are more likely to participate in oxidation reactions. The descriptions below for the most common and state-of-the-art photocatalytic driven processes are summarized in a previous review.[16] For further in-depth analysis of the mechanistic and kinetic overview of photocatalytic interactions for PFAS materials, the authors advise reading this article (Fig. 8).

3.2 Photo-oxidative degradation of PFCA *via* heterogeneous catalysts

Various mechanistic routes are proposed in the literature as to the actual degradation mechanism of perfluoroalkyl carboxylic acid (PFCA) in water *via* the photo-generated hole (h_{vb}^+) under UV light. The consensus on the mechanism involves the generated hole abstracting an electron from its surroundings forming a radical species. The competing mechanisms are for the h_{vb}^+ to either abstract the electron from hydroxyl anions (HO^-) in solution, producing hydroxyl radicals ($HO^\bullet$), or the h_{vb}^+ abstracts an electron from the PFAS head group, taking PFCA ($C_nF_{2n+1}COO^-$) as an example, and generates a PFCA radical ($C_nF_{2n+1}COO^\bullet$). In the case of hydroxyl radical formation, the radical attacks the acid head group, abstracting the hydrogen and transferring the radical species onto the carbonyl group, generating the PFCA radical.[48] However, such H-atom abstraction requires the headgroup of the PFCA to be protonated which is unlikely in the aqueous phase near neutral pH since the pK_a of PFCA is known to be very low. A surface coordination of PFCA however may cause the polar headgroup to be protonated. Nonetheless, of the two options, the experimental observations indicate that PFCA coordination onto the surface is the more influential pathway. This is due to an observed dependence on the PFCA chain length, which has been attributed to shorter chains being unable to adsorb onto the catalytic surface. As a result, the longer PFCA is degraded more quickly, and hence there is a chain length dependence in such degradation approaches.[49,50] Meanwhile, the hydroxyl radical flows freely through solution and has no such restriction based on chain length due to adsorption. Once the PFCA radical is formed, a variety of degradation pathways are proposed with the common result being a loss of one CF_2 group from the carbon chain length, producing CO_2 and HF as the end products. The resulting shorter chain PFCA ($C_{n-1}F_{2n-1}COO^-/C_{n-1}F_{2n-1}COOH$) then undergoes the degradation cycle again, removing a CF_2 group each time. Fig. 9 shows the proposed degradation mechanisms *via* the radical formation.

Regardless of the mechanism involved, the overall lifetime of photoexcited holes is crucial. A longer hole lifetime enhances the catalyst's ability to directly oxidize PFCA or water, thereby initiating the degradation mechanism. Therefore, improvements in photocatalysis, such as more efficient charge separation leading to prolonged hole lifetimes, are likely to enhance PFCA degradation.

When discussing PFCA degradation, it is important to note that chain shortening or other carbon–carbon bond breaking is insufficient for PFCA destruction, as those will result in PFCA with a shorter chain length. These shortened PFCA molecules are similarly detrimental to health and the environment but harder to detect and destroy. For true PFCA and other PFAS degradation, the carbon–fluorine bonds must be broken. This is one of the advantages of reduction over oxidation (section 3.3 Photo-reductive degradation of PFAS). Reduction pathways typically directly attack the carbon–fluorine bonds while oxidation pathways are chain shortening. Complete oxidation and mineralization are required for the desired result of complete PFAS destruction.[51]

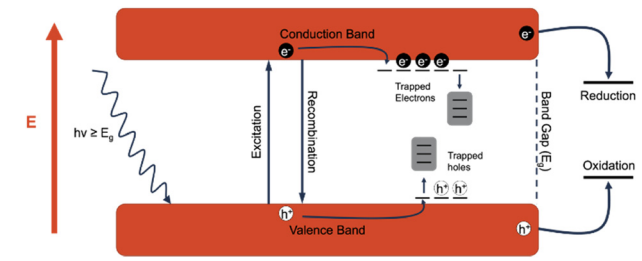

Fig. 8 Diagram depicting the absorbance of a photon in a semiconducting material, resulting in the generation of an exciton. The generated electron exists within the conduction band, whereas the hole exists within the valence band. By 'trapping' either the conduction band electron or valence hole, the lifetime of the generated exciton pair can be elongated. Generated electrons undergo reduction and generated holes undergo oxidation. This figure was created by the authors.

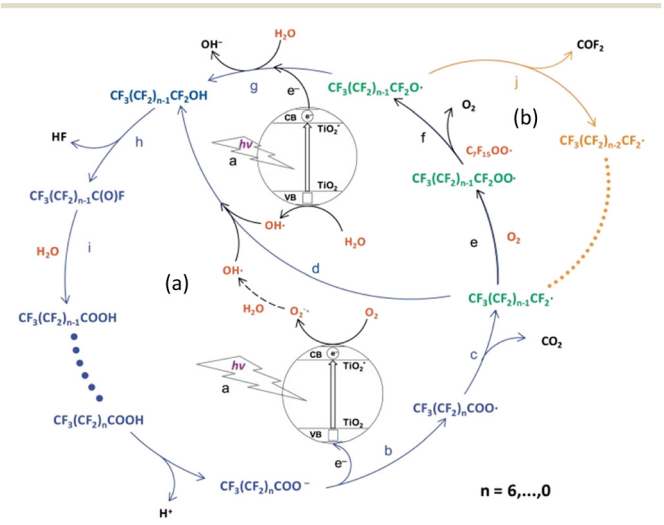

Fig. 9 Diagram of potential PFCA degradation pathways *via* radical generation. Photo-redox pathway (blue arrows (a)) and β-scission pathway (orange arrows (b)).[52] This image has been modified from its original publication.

3.2.1 Titanium dioxide. Titanium dioxide (TiO_2) is one of the most studied heterogeneous photocatalysts due to its low toxicity, abundance, and effectiveness for common applications such as the decomposition of H_2O. The extensive knowledge based on the material means that there are reliable options for modifications to suit the desired application. For example, it is well known that the band gap can be tuned through chemical modifications or the morphology can be altered for different adsorption capabilities. Additionally, titanium dioxide is an FDA approved food additive making it an attractive candidate for drinking water purification.[53]

Anatase TiO_2 has been studied for over a decade as a potential photocatalyst for PFCA degradation with little success. TiO_2 has been found to degrade PFCAs through charge transfer mediated oxidation as described above.[16,52,54–57] The main challenges regarding TiO_2 semiconductors are the short lifetime of the photogenerated exciton as well as the difficulty of oxidizing PFCAs with hydroxyl radicals at moderate pH values, the main reactive species generated from titania. Various methods of improving the exciton lifetime, and by extension photocatalytic capabilities, have been investigated *via* anatase TiO_2 compared to the baseline of P25 (P25 is a 3 : 1 ratio of the anatase to rutile phase), a combined phase of TiO_2. These improvements include nanostructured carbon supports, transition metal doping, and the formation of heterojunctions with other semiconductors.[16,57]

A study recently demonstrated that by adding noble metal nanoparticles to titania, the PFOA decomposition rate can be greatly increased. Silver, palladium, and platinum nanoparticles were deposited onto commercial P25 titania and the resultant photocatalytic properties were tested. The measured rate constants were up to 12.5 times higher in the case of the platinum modified nanoparticles than for the native P25. The increased reactivity was attributed to the metal nanoparticles acting as an electron sink, which increased the lifetimes of the exciton and, specifically, the holes, which participate in the decomposition. The authors also concluded that the catalysts became more effective as the work functions of the doped metals increased. This is because as the work function of the nanoparticle increases, the potential difference between the metal and the TiO_2 increases, allowing electrons to transfer from the TiO_2 to the metal faster.[58] This method of increasing decomposition is similar to the effect of adding electron scavengers to the reaction. Removing excess electrons from the catalyst will decrease recombination rates and make the photocatalyst more active. The addition of noble metal nanoparticles to TiO_2 allows for a similar effect that electron scavengers provide, without the need to add additional chemicals to the reaction, which could be undesirable when attempting to clean ground or drinking water.

One of the most successful examples of PFOA degradation with titanium dioxide was shown in a study by Wong and coworkers. A composite material of TiO_2 and boron nitride (BN) was made through a simple calcination procedure. This material was found to act as a type-II heterojunction semiconductor. This TiO_2–BN heterojunction yields a high concentration of holes on the BN with few electrons to recombine with, increasing recombination times and therefore overall efficiency of the exciton generation.[59] Further discussion of the effectiveness of BN photocatalysis for PFCA degradation can be found in section 3.2.4 Boron nitride. The use of carbon supports has been shown to improve TiO_2 photocatalytic degradation capabilities; however, the nature of the effect is disputed. While most reports agree that carbon support systems (such as graphene and carbon nanotubes) provide a route for the generated e_{cb}^- to 'escape' the exciton due to the conductive nature of the carbon support, other studies argue that the role of carbon is not related to its conductive properties but rather to its hydrophobic properties. The effect other hydrophobic supports had on the measured PFOA degradation by UV/TiO_2 photocatalysts was recently examined.[60] This work found that polytetrafluoroethylene (PTFE), polyethylene (PE), and graphene oxide (GO) all resulted in similar levels of PFOA degradation despite PTFE and PE being non-conductive. The authors postulated that rather than an electronic effect occurring *via* the nanostructured carbon supports, the hydrophobic nature of the carbon created zones of dehydration on the titania surface. These zones allowed for direct adsorption of PFCA to the titania surface and therefore facilitated faster charge transfer, as depicted in Fig. 10.

3.2.2 Indium oxide. Indium oxide (In_2O_3) semiconductors have been investigated as an alternative to TiO_2 for photocatalytic degradation. The primary motivation is that with In_2O_3, PFOA is able to bind to the surface metal sites in a bidentate fashion.[56] This bidentate formation results in a favoured direct exciton hole radical formation, rather than an intermediate pathway through hydroxyl radicals. Li *et al.* concluded that an In_2O_3 system generated substantially fewer hydroxyl radicals as compared to TiO_2, concluding that more exciton holes were directly generating radicals onto the PFOA carboxyl groups. The main benefit of this result is that the direct hole oxidation route has much faster kinetics to degrade the PFOA materials than *via* the hydroxyl radical intermediate resulting in more efficient degradation.

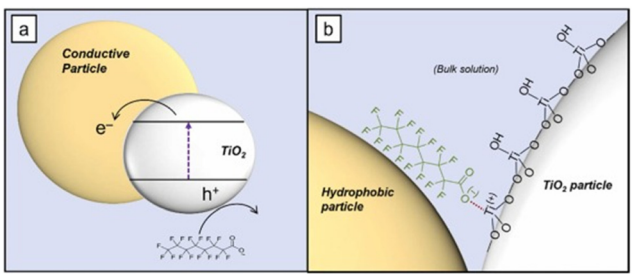

Fig. 10 Schematic depicting the hypothesized interaction between the hydrophobic graphene support and the TiO_2 semiconductor for PFOA oxidation.[60]

Analogous methods of enhancing the photocatalytic strength of TiO_2 have been investigated for In_2O_3. Carbon materials have been found to increase the photocatalytic activity of In_2O_3, where they are believed to act as transport materials for electrons, although it is possible that they act as hydrophobic supports as discussed within section 3.2.1 Titanium dioxide. The formation of heterojunctions has also been investigated, where the heterojunction allows for either the h_{vb}^+ or e_{cb}^- to be transported away resulting in an increase in exciton lifetime.[61] An example of this heterojunction is a recent effort that doped In into carbon-supported titanite nanotubes. This composite material showed 99% efficiency in PFOA degradation under optimal conditions.[62] The researchers attribute the success to the heterojunction, which facilitates electron transfer and stepwise defluorination, achieving ~60% defluorination after only 4 hours.

3.2.3 Gallium oxide. Another post-transition metal semiconductor investigated for photocatalytic PFOA degradation is gallium oxide (Ga_2O_3). Of the 5 stable structures Ga_2O_3 can form, monoclinic (β) Ga_2O_3 is known to be the most stable and is often the subject of photocatalytic studies. Similar to TiO_2, Ga_2O_3 has been found to exhibit different levels of photocatalytic activity with different morphologies. A study by Fu *et al.* found that at a pH of 3.0, the photocatalytic degradation of PFOA yielded $Ga_2O_3 > TiO_2 > CeO_2 > In_2O_3 >$ CdS. The authors determined that this result aligned with increasing band gap energies (Ga_2O_3) 4.57 eV > (TiO_2) 3.14 eV > (CeO_2) 2.93 eV > (In_2O_3) 2.80 eV > (CdS) 2.42 eV. The authors deemed that the initial pH and quantum yield were less indicative to the resulting order.[63]

3.2.4 Boron nitride. Researchers tested the photocatalytic activity of boron nitride (BN), a known semiconductor, compared to that of the standard P25.[64] They found that the presence of BN would decrease the concentration of PFOA when irradiated with 254 nm light. While the band gap of BN is around 6 eV and is therefore considered an electrical insulator and should not be excited *via* UV radiation,[65] the study determined that under similar conditions, the BN outperformed the P25 in its ability to decompose PFOA and its subsequent C_3–C_7 by-products. The authors attributed this ability to generate the required exciton pair for radical formation to defects within the hexagonal BN structure. By introducing more edge sites and vacancies *via* ball milling, the authors showed an increase in PFOA degradation rates from 0.24 to 0.44 mg of PFOA L^{-1} min^{-1}, supporting the notion that defect sites were indeed enabling the activation of excitons on the BN surface.

As previously mentioned, the addition of BN to TiO_2 was also found to improve photocatalytic activity *via* the formation of a type-II heterojunction. A type-II heterojunction means that the band gaps of the conjoined materials have an overlap, which allows excited electrons to go from the lower energy band gap into the higher energy band gap to prevent recombination. The defect sites in BN act as a secondary conduction band, with a much lower band gap than BN has natively. However, even with defect sites, the BN has a band gap that is considerably higher than other semiconductors such as TiO_2. This is evident by the fact that BN can be excited under higher energy ultraviolet C radiation (254 nm) but not ultraviolet A (365 nm). The benefit that the composite heterojunction provides is in irradiating with UV-C, electrons are excited in both materials and are then transferred to the lower energy conduction band of TiO_2, whereas the holes are transferred to the higher energy valence band of the BN. This yields a high concentration of holes on the BN with few electrons to recombine with.[59]

In a later study, it was found that BN is a superior active site for oxidation of PFCAs due to its high hydrophobicity, which promotes PFCA adsorption and prevents formation of hydroxyl radicals, which are less effective at oxidizing PFOA.[66]

3.2.5 Fe-exchanged zeolites. A recent investigation found that certain metal ion-exchanged zeolites were capable of PFOA adsorption and photodegradation. The H^+ ions in the zeolites were exchanged with different metal ions, such as Fe^{2+}. Among the various zeolites tested in their experiments, Fe-exchanged beta (BEA) zeolites were found to be the most effective for PFOA degradation. Most specifically, Fe-BEA35 was the morphology and 1.26 wt% Fe was the iron content they identified as the most effective. These zeolites have iron atoms present both externally and internally, and the researchers identified the internal iron sites as being effective for adsorbing PFOA in concentrations in the range of 8 to 20 μg L^{-1} with an adsorption coefficient (K_d) of up to 105 L kg^{-1}. Once the material was excited, photo-induced holes were able to oxidize the bound PFOA in the same mechanism as previously discussed photocatalysts. Notably, this material is excited by light in the UV-A range, the lower energy end of the UV spectrum. The material performed well, with 95% PFOA degradation within 8 hours, and 99.9% degradation and a 44% defluorination ratio were achieved within 24 hours. However, the researchers found a notable difference in the adsorption of linear PFOA *versus* branched chain isomers, with the branched chain isomers being only barely adsorbed after 24 hours. They attribute this to the branched chain isomers being unable to enter the narrow pores of the material due to their size. It is reasonable to assume that photocatalysts which have adsorption sites on the outside of the material may therefore be better suited to degrade the variety of PFCA isomers found under environmental conditions. However, if the pore environment is the main factor affecting the efficiency of this catalyst, perhaps wider pores may be able to accommodate the branched chain isomers but still create the correct reactive chemical environment. Future research directions include examining different morphologies with different pore sizes and exchanging different transition metals into zeolites to elucidate which of these factors are the most important in the material success.[67]

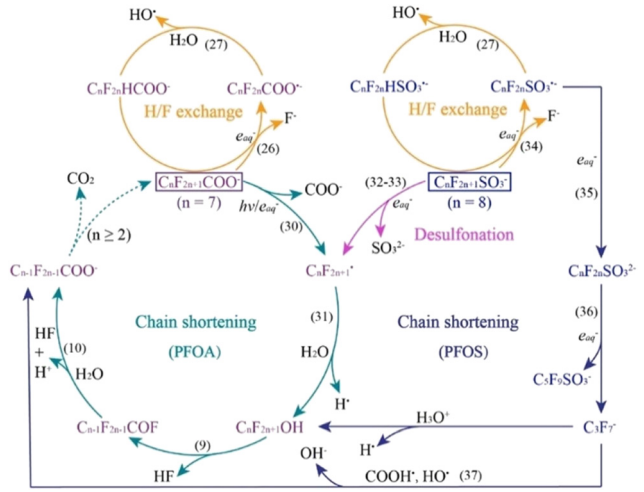

Fig. 11 Proposed cyclic pathways of PFOA and PFOS degradation *via* aqueous electrons. Numbers in parentheses (*e.g.* (26), (31), *etc.*) correspond to equations within the original paper.[16]

3.3 Photo-reductive degradation of PFAS

In contrast to the oxidative processes described above, photo-reductive pathways for PFAS materials involve the generation of reducing radicals *via* an activation source such as UV light and reducing compounds such as sulfites and sulfides.[16,68] These reducing radicals mainly occur as either hydrated electrons (e_{aq}^-) and hydrogen atoms (H$^\bullet$), with side-products from reducing agents occurring as well ($SO_3^{\bullet-}$ in the case of sulfite). The hydrated electron is the most studied reducing radical due to its strong reducing power and is found to cleave the PFAS molecule at the α-CF bond. This cleavage can occur due to the reduction potential of the C–F bond ($E <$ −2.7 V) being lower than that of the e_{aq}^- (E = −2.9). Once the α-site cleavage is instigated, cyclic stepwise degradation of the PFAS molecule occurs as shown in Fig. 11. Unlike the oxidative degradation pathways where the polar headgroup loses an electron, the reductive degradation mechanisms are shown to be more complicated. A recent study showed that the defluorination due to the reactivity of PFAS with a hydrated electron depends on the polar head group.[69] In the case of carboxylates, the defluorination occurs at the alpha-carbon (the carbon next to the carboxylic acid), whereas the defluorination occurs at the middle of the perfluoroalkyl chain in the case of the sulfonate head group. This mechanistic computational study aligns well with the known observed rate constants of PFAS with hydrated electrons in constant irradiation experiments in the aqueous phase.[70–73] Series of other studies also demonstrated the use of C–F bond dissociation energies as a marker to probe the feasibility of reductive degradation of PFAS. The defluorination event is followed by H/F exchange as shown in Fig. 11. Molecular mechanisms involved in reductive degradation of PFAS are less established when compared to the oxidative degradation pathways. Nevertheless, since the reduction of PFAS is energetically more feasible when compared to oxidation, chemical reduction is a more attractive technique. In terms of scaling up of photocatalytic reductive degradation approaches for PFAS, one must pay attention to the co-constituents which can also act as non-target scavengers of hydrated electrons as demonstrated by a recent study.[74,75]

4. Future outlooks

4.1 Hydroxyl radical and TiO_2 debate

Within the PFAS photocatalyst literature, there is an ongoing discussion on the effectiveness of the TiO_2 material as a photocatalyst for oxidative degradation of PFAS, typically targeting PFOA. A paper by Li *et al.* compared the performance of TiO_2 to that of In_2O_3 for PFOA degradation *via* UV-light irradiation.[56] The paper claims that TiO_2 decomposes PFOA by generating hydroxyl radicals which in turn react with PFOA, and that the interaction between HO$^\bullet$ and PFOA is not favourable. The paper goes on to claim that In_2O_3 is able to perform direct radicalization of PFOA *via* favourable surface interactions, and showed that In_2O_3 degrades approximately 5 times more PFOA than TiO_2 after 4 hours of irradiation under 254 nm UV light (80% and 15.9%, respectively).[56]

A paper by Javed *et al.* attempted to show the effectiveness of HO$^\bullet$ for PFOA degradation.[76] In the study, the authors use H_2O_2 irradiated with UV light to form HO$^\bullet$ to act as the oxidizing agent. The authors concluded that compared to photolysis, the process of PFOA degradation *via* direct UV irradiation, the UV + H_2O_2 system showed no enhancement and that at higher concentrations, it hampered PFOA degradation.[76]

Bouteh *et al.* analysed the impact of graphene oxide (GO) supports on TiO_2 and its photocatalytic degradation of PFCA including PFOA. The authors determined that due to binding of hydroxyl groups onto the TiO_2 surface, the ability to bind PFCA close enough for direct photooxidative reactions was hampered. Contrary to some published reports, which state that GO supports increase the lifespan of generated excitons by creating pathways for generated electrons, the authors compared other non-conductive hydrophobic supports and concluded that the hydrophobicity of the GO is the defining factor in improving the TiO_2 activity. The paper claims that the hydrophobic supports are able to retain PFAS near the surface of TiO_2 sufficiently long enough for a photooxidative process to occur and alludes to the low performance of TiO_2 photocatalysts.[60]

Future research involving different support materials that bind more strongly to PFAS is required to elucidate the role of the support. One possibility is measuring the degradation of different length PFCA, because of the chain length dependence of this hydrophobic interaction. If there is a more pronounced chain length dependence with the supporting material, then it is likely that the hydrophobic interaction is the main driving force, and *vice versa*. Alternatively, it may be possible using advanced surface

analysis techniques to examine how PFAS coordinates to the surfaces in these systems.

In the three example publications (*vide supra*), the photocatalytic activity of TiO_2 is viewed as poor, with points of contention including the ineffectiveness of generated $HO^{\bullet}$ for degrading PFOA, the slow surface-to-PFOA direct oxidation pathways, and the low binding affinity of PFCAs onto the catalyst surface. Taken in isolation, these papers paint a clear picture that TiO_2, typically used in its P25 form, is inefficient at degrading PFAS compounds.

A paper by Fu *et al.* attempted to categorically compare the commonly tested semiconductors and their ability to degrade PFOA. In this paper, the authors compared Ga_2O_3, In_2O_3, CeO_2, TiO_2, and CdS, with all materials tested under the same PFOA starting concentration, temperature, initial pH, and UV irradiation conditions. The results of the study indicated that the highest impact of effectiveness of PFOA degradation after 10 hours mirrored the size of the semiconductor band gap, resulting in the following ranking from the most to least efficient: $Ga_2O_3 > TiO_2 > CeO_2 > In_2O_3 >$ CdS. Here, the effectiveness of TiO_2 was measured to be 84%, while In_2O_3 was measured to degrade 20% of the initial PFOA.[63] These results are nearly in direct opposition of those of Li *et al.*

An important factor mentioned in both papers is the pH. Li *et al.* mentioned that at pH < 2, the TiO_2 activity for PFOA degradation is increased significantly, with their experiments run under pH conditions of 3.8. One may argue that at pH $<$ 2, some fraction of PFOA will be protonated, thereby undergoing oxidation *via* electrons in the conduction band as weak as *via* H-atom abstraction by $HO^{\bullet}$. However, Fu *et al.* ran their experiments with an initial pH of 3.0 ± 0.2, resulting in a much higher activity in the TiO_2 semiconductor compared to Li *et al.* While this is an indicator of the effect of pH on TiO_2 photocatalytic activity, it is important to note that these two investigations had other variables in their experimental setup. Fu *et al.* conducted their experiments with a 32 W low-pressure UV lamp with 254 nm light and a starting PFOA concentration of 50 ng L^{-1}. Li *et al.* ran their experiments with a 23 W low-pressure UV lamp with 254 nm light and a starting PFOA concentration of 100 μmol L^{-1}, or 41 mg L^{-1}, which is 6 orders of magnitude greater than Fu *et al.* The reasoning behind this large concentration was to reduce the impact of In_2O_3 adsorption onto PFOA, reducing activity.

The lack of surface area measurements for complete comparison has been noted in many studies. We believe that by adding this lens to compare various photocatalysts, a more complete picture can be drawn. Until differences in surface areas can be removed as a potential factor in PFAS degradation performance, a conclusive statement on the effectiveness of the said photocatalysts will also be up for debate.

A recent paper by Carre-Burritt *et al.* attempted to determine the effectiveness of PFCA destruction *via* generated $HO^{\bullet}$ radicals in an aqueous solution using computational methods. They noted that as the reduction potential ($E°$) of the ($HO^{\bullet}/HO^{-}$) couple is around 1.9 V compared to the range of ($PFCA^{\bullet}/PFCA^{-}$) $E°$ of 2.2–2.5 V, the ability of the $HO^{\bullet}$ radical to oxidize PFCA compounds is unfavoured. At pH 0 however, the $E°$ of ($HO^{\bullet}$, H^{+}/H_2O) is noted to be around 2.73 V, indicating that hydroxyl radicals generated at lower pH should have a thermodynamically favoured reaction with PFCA compounds. The paper shows that within a range of pH −1.0 to 1.5, their chosen PFCA, perfluorobutanoic acid, was more effectively destroyed at lower pH values and that a significant portion of the degradation occurred *via* H-abstraction.[48]

In general, the effectiveness of hydroxyl radicals and by extension TiO_2 photocatalysts is less than that of other available photocatalysts. However, the key takeaway we would like to provide is that the efficiency can be increased significantly *via* low and ultralow pH and thereby would provide a more accurate comparison of P25 activity as a baseline.

4.2 Other post-transition metals as semi-conductor photocatalysts

Ga, In and Bi are three post-transition metals whose oxides are commonly investigated as potential semiconductors for oxidative PFAS degradation. These metals are found in groups 13 and 15. As elements within the same group are often found to have similar chemical activity, it is worth noting that Tl, As, and Sb and their respective oxides are not included in investigations into light driven semiconductor technology for PFAS degradation. While these elements are known to be toxic, their potential uses in PFAS destruction are worthy of further attention particularly as a means to gain deeper fundamental insights. Recent work studying SbO_3 supports for a TiO_2 photooxidative system was published and showed results of increased PFAS degradation when compared to standalone TiO_2. The generated heterojunction of Sb_2O_3/TiO_2 resulted in a removal of 81.83% of initial PFOA compared to the standalone P25 removal of 32.3% and mesoporous TiO_2 removal of 55.9% of initial PFOA.[57]

4.3 Effect of porosity on PFAS photocatalysis

An underexplored tool for PFAS photodegradation is the use of porous catalysts. One major issue with the use of photocatalysts for PFCA degradation is that the oxidation product is the same PFCA but one chain length shorter. This results in total mineralization becoming more difficult as each shorter chain PFCA is less prone to oxidation. Oxidation becomes more difficult with shorter chains because there is a chain length dependence in PFOA adsorption onto most catalysts. And so as the PFCA has chain lengths removed, it becomes more difficult to adsorb and undergo oxidation. A possible solution to this problem would be to use porous photocatalysts. The effect of the pore would be to keep the oxidized PFCA adsorbed within the pore volume, preventing desorption and bypassing the issue of needing to readsorb.

However, there are inherent issues with using a porous photocatalyst. Namely, as a photocatalyst interacts with light primarily on the surface, it becomes difficult for charge carriers to be activated in the bulk, where the majority of the surface area is in a porous material. Yet there are a plurality of effective porous photocatalysts in the literature which are able to take advantage of the drastically increased surface area and mass transfer that the materials provide.[77,78]

5. Conclusions

This review covers aspects of the light-driven technologies of photocatalysis and plasmonic processes, concerning both how light enables their effects and how they are used in relation to PFAS. The field of PFAS remediation research is vast however, and many knowledge gaps and future challenges still need to be addressed. Some of these challenges are identified below:

- Almost all papers performing initial testing on photocatalytic degradation of PFCA focus on PFOA as their primary PFCA. While the PFOA molecule is known to be toxic, well studied for comparison, and is a known recalcitrant molecule within the PFCA family, some techniques which have shown promise for breaking down PFOA have shown no to little effect on PFOS. As PFOA and PFOS are both legacy PFAS with very low limits of allowed concentrations within drinking water, a more diversified spread of PFAS degradation testing will be beneficiary for narrowing down potential large-scale implementations for effectively breaking down different PFAS molecules.

- While research has compared the photocatalytic capabilities of various materials, no standard baseline has been determined for accurate photocatalytic testing. While LC-MS is typically considered as the most reliable technique, due to the relatively high amount of user training and analyte set-up required, many researchers have sought out other techniques such as F^- ion probing. Certain concerns have been raised on potential false-positive readings of other anions within solution, and in porous systems, the F^- ions can be trapped within the system and therefore read as false-negatives. Reliable and facile benchtop testing of PFAS degradation would allow for more streamlined comparisons of degradation results.

- When PFAS degradation research is reported, the parameters which are given to determine catalytic effectiveness can vary greatly. When reporting catalytic improvement, authors tend to compare their material to P25, which has been determined with some consensus to be a baseline photocatalyst. However, as P25 will be active only in lower pH ranges, tests run at a higher pH will result in an increase in perceived activity of the new material, as P25 is essentially not able to perform. Not only that, but when comparisons are made, rather than detailing catalyst reaction rates, some papers compare their material to their P25 *via* percentages and magnitude of activity noted. While such statements can aid in the discussion of improvements found within novel materials, without having a baseline in which P25 is active (ergo a high pH and low pH comparison), any claims made about the relative activity of the novel photocatalyst fall short. Additionally, we believe that an agreement of set parameters, including pH, light intensity, PFAS loading, exposure time, and others, should be established for PFAS photodegradation to ensure that just comparisons can be made throughout the literature.

- Most testing done on both light-driven technologies tends to be conducted under only ideal conditions. Initial testing for advancements being done in a simple solution and under ideal conditions is logical, as it allows for more comprehensive result analysis and comparison to other studies done in the literature. However, by not following up on these tests with more complex matrix analysis, certain capabilities of novel materials may be overstated as their functionality under real-world conditions is not expressed. Real world PFAS contaminated systems will have multiple types of PFAS and can include a wide range of non-PFAS type organic pollutants, as well as other contaminants. Only by adding some rudimentary testing with a more complex matrix can the applications of these materials be judged for environmental remediation.

Data availability

No primary research results, software or code have been included and no new data were generated or analysed as part of this review.

Author contributions

F. R. A. S. and S. E. M. wrote the original draft, provided the literature study and formal analysis, and revised the manuscript. B. G. T., S. V. and R. M. R. acquired funding for the project, management, revision of the manuscript and conceptualization. M. R. D. provided analysis and revision of the manuscript.

Conflicts of interest

There are no conflicts to declare.

Acknowledgements

The authors thank the Army Core of Engineers (Fund number: W912HZ-23-2-0009) for funding this work. The team also acknowledges support from PFAS@Mines.

Notes and references

1 J. N. Meegoda, B. Bezerra De Souza, M. M. Casarini and J. A. Kewalramani, *Int. J. Environ. Res. Public Health*, 2022, **19**, 16397.
2 S. Yadav, I. Ibrar, R. A. Al-Juboori, L. Singh, N. Ganbat, T. Kazwini, E. Karbassiyazdi, A. K. Samal, S. Subbiah and A. Altaee, *Chem. Eng. Res. Des.*, 2022, **182**, 667–700.

3 M. P. Purdue, J. Rhee, H. Denic-Roberts, K. A. McGlynn, C. Byrne, J. Sampson, J. C. Botelho, A. M. Calafat and J. Rusiecki, *Environ. Health Perspect.*, 2023, **131**, 077007.
4 J. Rhee, K. H. Barry, W.-Y. Huang, J. N. Sampson, J. N. Hofmann, D. T. Silverman, A. M. Calafat, J. C. Botelho, K. Kato, M. P. Purdue and S. I. Berndt, *Environ. Res.*, 2023, **228**, 115718.
5 V. C. Chang, J. Rhee, S. I. Berndt, S. C. Moore, N. D. Freedman, R. R. Jones, D. T. Silverman, G. L. Gierach, J. N. Hofmann and M. P. Purdue, *Int. J. Cancer*, 2023, **153**, 775–782.
6 R. R. Jones, J. M. Madrigal, R. Troisi, H.-M. Surcel, H. Öhman, J. Kivelä, H. Kiviranta, P. Rantakokko, J. Koponen, D. N. Medgyesi, K. A. McGlynn, J. Sampson, P. S. Albert and M. H. Ward, *JNCI, J. Natl. Cancer Inst.*, 2023, djad261.
7 J. T. Szilagyi, V. Avula and R. C. Fry, *Curr. Environ. Health Rep.*, 2020, **7**, 222–230.
8 C. R. Stein, D. A. Savitz, B. Elston, P. G. Thorpe and S. M. Gilboa, *Reprod. Toxicol.*, 2014, **47**, 15–20.
9 Y. Li, T. Fletcher, D. Mucs, K. Scott, C. H. Lindh, P. Tallving and K. Jakobsson, *Occup. Environ. Med.*, 2018, **75**, 46–51.
10 G. F. Peaslee, J. T. Wilkinson, S. R. McGuinness, M. Tighe, N. Caterisano, S. Lee, A. Gonzales, M. Roddy, S. Mills and K. Mitchell, *Environ. Sci. Technol. Lett.*, 2020, **7**, 594–599.
11 Wisconsin Department of Health Services, Chemicals: Perfluoroalkyl and Polyfluoroalkyl (PFAS) Substances, **https://www.dhs.wisconsin.gov/chemical/pfas.htm**, (accessed 31 January 2024).
12 Wisconsin Department of Natural Resources, PFAS-Containing Firefighting Foam, **https://dnr.wisconsin.gov/topic/PFAS/AFFF.html**, (accessed 31 January 2024).
13 L. G. T. Gaines, *Am. J. Ind. Med.*, 2023, **66**, 353–378.
14 I. Najm, B. Gallagher, N. Vishwanath, N. Blute, A. Gorzalski, A. Feffer and S. Richardson, *AWWA Water Sci.*, 2021, **3**, e1245.
15 Y. Wang, Y. Ji, V. Tishchenko and Q. Huang, *Chemosphere*, 2023, **311**, 137004.
16 F. Liu, X. Guan and F. Xiao, *J. Hazard. Mater.*, 2022, **439**, 129580.
17 K. Kabra, R. Chaudhary and R. L. Sawhney, *Ind. Eng. Chem. Res.*, 2004, **43**, 7683–7696.
18 A. D. Dotson, C. E. Rodriguez and K. G. Linden, *J. AWWA*, 2012, **5**, E318–324.
19 *FACT SHEET PFOA & PFOS Drinking Water Health Advisories*, US Environmental Protection Agency, 2016.
20 Biden-Harris Administration Finalizes First-Ever National Drinking Water Standard to Protect 100M People from PFAS Pollution, **https://www.epa.gov/newsreleases/biden-harris-administration-finalizes-first-ever-national-drinking-water-standard**.
21 A. E. Cetin, A. F. Coskun, B. C. Galarreta, M. Huang, D. Herman, A. Ozcan and H. Altug, *Light: Sci. Appl.*, 2014, **3**, e122.
22 T. Mueller, A. C. Ferrari, F. Koppens, F. Xia and X. Xu, *IEEE J. Sel. Top. Quantum Electron.*, 2014, **20**, 0200103.
23 J.-H. Park, Y.-W. Cho and T.-H. Kim, *Biosensors*, 2022, **12**, 180.
24 M. Alavirad, S. S. Mousavi, L. Roy and P. Berini, *Opt. Express*, 2013, **21**, 4328.
25 R. Pitruzzella, F. Arcadio, C. Perri, D. Del Prete, G. Porto, L. Zeni and N. Cennamo, *Chemosensors*, 2023, **11**, 211.
26 H. B. Lamichhane and D. W. M. Arrigan, *Curr. Opin. Electrochem.*, 2023, **40**, 101309.
27 R. B. Clark and J. E. Dick, *ACS Sens.*, 2020, **5**, 3591–3598.
28 S. P. Sahu, S. Kole, C. G. Arges and M. R. Gartia, *ACS Omega*, 2022, **7**, 5001–5007.
29 G. I. Janith, H. S. Herath, N. Hendeniya, D. Attygalle, D. A. S. Amarasinghe, V. Logeeshan, P. M. T. B. Wickramasinghe and Y. S. Wijayasinghe, *J. Pharm. Biomed. Anal. Open*, 2023, **2**, 100019.
30 J. Pollet, F. Delport, K. P. F. Janssen, K. Jans, G. Maes, H. Pfeiffer, M. Wevers and J. Lammertyn, *Biosens. Bioelectron.*, 2009, **25**, 864–869.
31 J. Jing, K. Liu, J. Jiang, T. Xu, S. Wang, J. Ma, Z. Zhang, W. Zhang and T. Liu, *Photonics Res.*, 2022, **10**, 126.
32 R. F. Menger, E. Funk, C. S. Henry and T. Borch, *Chem. Eng. J.*, 2021, **417**, 129133.
33 H. Ryu, B. Li, S. De Guise, J. McCutcheon and Y. Lei, *J. Hazard. Mater.*, 2021, **408**, 124437.
34 A. U. Rehman, M. Crimi and S. Andreescu, *Trends Environ. Anal. Chem.*, 2023, **37**, e00198.
35 S. V. Boriskina, H. Ghasemi and G. Chen, *Mater. Today*, 2013, **16**, 375–386.
36 M. E. King, C. Wang, M. V. Fonseca Guzman and M. B. Ross, *Chem Catal.*, 2022, **2**, 1880–1892.
37 C. M. Miyazaki, F. M. Shimizu and M. Ferreira, in *Nanocharacterization Techniques*, Elsevier, 2017, pp. 183–200.
38 E. Southerland and L. S. Birnbaum, *Environ. Sci. Technol.*, 2023, **57**, 7103–7105.
39 V. Amendola, R. Pilot, M. Frasconi, O. M. Maragò and M. A. Iatì, *J. Phys.: Condens. Matter*, 2017, **29**, 203002.
40 M. Ahlawat, D. Mittal and V. Govind Rao, *Commun. Mater.*, 2021, **2**, 114.
41 H. Wei, S. K. Loeb, N. J. Halas and J.-H. Kim, *Proc. Natl. Acad. Sci. U. S. A.*, 2020, **117**, 15473–15481.
42 Z. Zhang, C. Zhang, H. Zheng and H. Xu, *Acc. Chem. Res.*, 2019, **52**, 2506–2515.
43 Z. Bian, T. Tachikawa, P. Zhang, M. Fujitsuka and T. Majima, *J. Am. Chem. Soc.*, 2014, **136**, 458–465.
44 A. Dey, A. Mendalz, A. Wach, R. B. Vadell, V. R. Silveira, P. M. Leidinger, T. Huthwelker, V. Shtender, Z. Novotny, L. Artiglia and J. Sá, *Nat. Commun.*, 2024, **15**, 445.
45 I. García-García, E. C. Lovell, R. J. Wong, V. L. Barrio, J. Scott, J. F. Cambra and R. Amal, *ACS Sustainable Chem. Eng.*, 2020, **8**, 1879–1887.
46 J. N. G. Stanley, I. García-García, T. Perfrement, E. C. Lovell, T. W. Schmidt, J. Scott and R. Amal, *Chem. Eng. Sci.*, 2019, **194**, 94–104.
47 Y. F. Zhu, B. Xie, J. A. Yuwono, P. Kumar, A. S. Sharma, M. P. Nielsen, A. Bendavid, R. Amal, J. Scott and E. C. Lovell, *EES Catal.*, 2024, **2**, 834–849.
48 A. Carre-Burritt, C. Amador and S. Vyas, Aqueous PFCA Destruction by Hydroxyl Radical at Low pH: A Putative

H-atom Abstraction Mechanism, *ChemRxiv*, 2022, preprint, DOI: 10.26434/chemrxiv-2022-64bzw.
49 Y. Wang, R. Pierce, H. Shi, C. Li and Q. Huang, *Environ. Sci.: Water Res. Technol.*, 2020, **6**, 144–152.
50 L. Li, Y. Wang and Q. Huang, *ACS ES&T Eng.*, 2021, **1**, 1737–1744.
51 S. C. E. Leung, P. Shukla, D. Chen, E. Eftekhari, H. An, F. Zare, N. Ghasemi, D. Zhang, N.-T. Nguyen and Q. Li, *Sci. Total Environ.*, 2022, **827**, 153669.
52 M. Sansotera, F. Persico, V. Rizzi, W. Panzeri, C. Pirola, C. L. Bianchi, A. Mele and W. Navarrini, *J. Fluorine Chem.*, 2015, **179**, 159–168.
53 J. Schneider, M. Matsuoka, M. Takeuchi, J. Zhang, Y. Horiuchi, M. Anpo and D. W. Bahnemann, *Chem. Rev.*, 2014, **114**, 9919–9986.
54 S. C. Panchangam, A. Y.-C. Lin, K. L. Shaik and C.-F. Lin, *Chemosphere*, 2009, **77**, 242–248.
55 B. Xu, M. B. Ahmed, J. L. Zhou, A. Altaee, M. Wu and G. Xu, *Chemosphere*, 2017, **189**, 717–729.
56 X. Li, P. Zhang, L. Jin, T. Shao, Z. Li and J. Cao, *Environ. Sci. Technol.*, 2012, **46**, 5528–5534.
57 X. Yao, J. Zuo, Y.-J. Wang, N.-N. Song, H.-H. Li and K. Qiu, *Front. Chem.*, 2021, **9**, 690520.
58 M. Li, Z. Yu, Q. Liu, L. Sun and W. Huang, *Chem. Eng. J.*, 2016, **286**, 232–238.
59 L. Duan, B. Wang, K. N. Heck, C. A. Clark, J. Wei, M. Wang, J. Metz, G. Wu, A.-L. Tsai, S. Guo, J. Arredondo, A. D. Mohite, T. P. Senftle, P. Westerhoff, P. Alvarez, X. Wen, Y. Song and M. S. Wong, *Chem. Eng. J.*, 2022, **448**, 137735.
60 E. Bouteh, M. J. Bentel and E. L. Cates, *J. Hazard. Mater.*, 2023, **453**, 131437.
61 J. Paul Guin, J. A. Sullivan and K. R. Thampi, *ACS Eng. Au*, 2022, **2**, 134–150.
62 J.-M. Arana Juve, F. Li, Y. Zhu, W. Liu, L. D. M. Ottosen, D. Zhao and Z. Wei, *Chemosphere*, 2022, **300**, 134495.
63 C. Fu, X. Xu, C. Zheng, X. Liu, D. Zhao and W. Qiu, *Environ. Geochem. Health*, 2022, **44**, 2943–2953.
64 L. Duan, B. Wang, K. Heck, S. Guo, C. A. Clark, J. Arredondo, M. Wang, T. P. Senftle, P. Westerhoff, X. Wen, Y. Song and M. S. Wong, *Environ. Sci. Technol. Lett.*, 2020, **7**, 613–619.
65 M. Kim, A. Peeples, H. Estrada, S. Fowler, L. Chiang, J. Morgan, M. Doganay, B. Walls, B. Wang, J. C. Samba and M. S. Wong, in *2021 Waste-management Education Research Conference (WERC)*, IEEE, Las Cruces, NM, USA, 2021, pp. 1–7.
66 B. Wang, Y. Chen, J. Samba, K. Heck, X. Huang, J. Lee, J. Metz, M. Bhati, J. Fortner, Q. Li, P. Westerhoff, P. Alvarez, T. P. Senftle and M. S. Wong, *Chem. Eng. J.*, 2024, **483**, 149134.
67 L. Qian, H. Zhao, A. Schierz, K. Mackenzie and A. Georgi, *ACS ES&T Eng.*, 2024, **4**, 748–757.
68 O. C. Olatunde, A. T. Kuvarega and D. C. Onwudiwe, *Heliyon*, 2020, **6**, e05614.
69 D. J. Van Hoomissen and S. Vyas, *Environ. Sci. Technol. Lett.*, 2019, **6**, 365–371.
70 R. Tenorio, A. C. Maizel, C. E. Schaefer, C. P. Higgins and T. J. Strathmann, *Environ. Sci. Technol.*, 2022, **56**, 14774–14787.
71 R. Tenorio, J. Liu, X. Xiao, A. Maizel, C. P. Higgins, C. E. Schaefer and T. J. Strathmann, *Environ. Sci. Technol.*, 2020, **54**, 6957–6967.
72 C. K. Amador, H. Cavalli, R. Tenorio, H. Tetu, C. P. Higgins, S. Vyas and T. J. Strathmann, *Environ. Sci. Technol.*, 2023, **57**, 7849–7857.
73 C. K. Amador, D. J. Van Hoomissen, J. Liu, T. J. Strathmann and S. Vyas, *Chemosphere*, 2023, **311**, 136918.
74 C. K. Amador, H. Cavalli, R. Tenorio, H. Tetu, C. P. Higgins, S. Vyas and T. J. Strathmann, *Environ. Sci. Technol.*, 2023, **57**, 7849–7857.
75 C. K. Amador, S. Vyas and T. J. Strathmann, *Environ. Sci. Technol.*, 2024, acs.est.3c10584.
76 H. Javed, C. Lyu, R. Sun, D. Zhang and P. J. J. Alvarez, *Chemosphere*, 2020, **247**, 125883.
77 A. A. Ismail and D. W. Bahnemann, in *Environmental Photochemistry Part III*, ed. D. W. Bahnemann and P. K. J. Robertson, Springer Berlin Heidelberg, Berlin, Heidelberg, 2015, vol. 35, pp. 221–266.
78 H. Mao, F. Zhang, M. Du, L. Dai, Y. Qian and H. Pang, *Ceram. Int.*, 2021, **47**, 25177–25200.